Supporting Information

Unraveling the ultra-low threshold stimulated emission from CdZnS/ZnS quantum dot and enabling high-Q microlasers

Yue Wang,[1] *Kah Ee Fong,*[2] *Shancheng Yang,*[1] *Van Duong Ta,*[1] *Yuan Gao,*[1] *Zeng Wang,*[1,3] *Venkatram Nalla,*[3] *Hilmi Volkan Demir,*[1,2,3,4]* *Handong Sun*[1,3]*

1 Division of Physics and Applied Physics, School of Physical and Mathematical Sciences, Nanyang Technological University, Singapore 637371, Singapore

2 School of Electrical and Electronic Engineering, Luminous! Center of Excellence for Semiconductor Lighting and Displays, Nanyang Technological University, Nanyang Avenue, Singapore 639798, Singapore

3 Centre for Disruptive Photonic Technologies (CDPT), Nanyang Technological University, Singapore, Singapore 637371, Singapore

4 Department of Electrical and Electronics Engineering, Department of Physics,and UNAM-National Nanotechnology Research Center, Bilkent University, Bilkent, Ankara

* HDSun@ntu.edu.sg and HVDemir@ntu.edu.sg

Figure S1 shows the energy-dispersive X-ray (EDX) spectrum of CdZnS core, from which the atomic percentages of Cd and Zn are determined to be ~22% and ~28%. Therefore, the CdZnS QDs adopted here can also be referred as $Cd_{0.44}Zn_{0.56}S$. The peaks of Carbon and Cu come from the substrate - the carbon coated copper mesh.

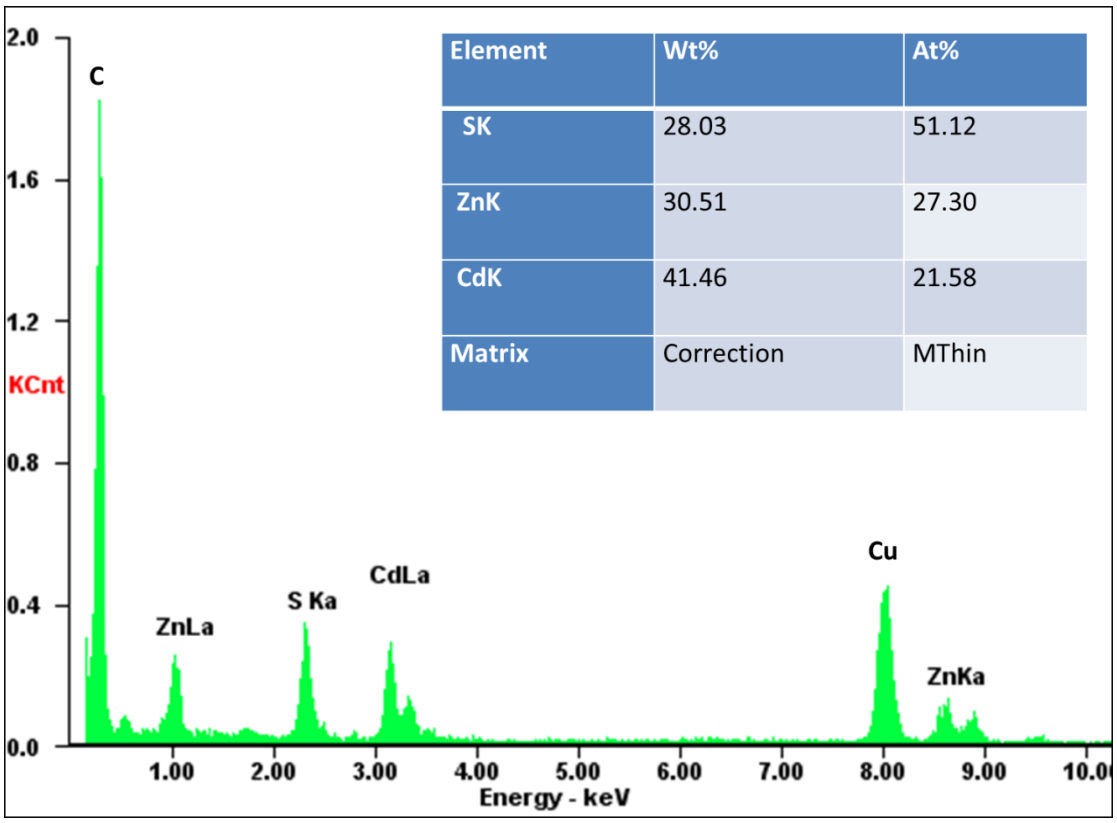

Element	Wt%	At%
SK	28.03	51.12
ZnK	30.51	27.30
CdK	41.46	21.58
Matrix	Correction	MThin

Figure S1. Energy-dispersive X-ray spectrum of CdZnS core, revealing the atomic percentages of Cd and Zn of ~22 and ~28, respectively.

Figure S2 shows the high resolution TEM images of CdZnS core (top), CdZnS/ZnS SS (middle) and CdZnS/ZnS AS (bottom) CQDs. For the thin-shelled CdZnS/ZnS SS QDs, due to the small lattice mismatch (~4%) between $Cd_{0.44}Zn_{0.56}S$ core and ZnS shell and the epitaxial growth of shell [1, 2], there is no observable boundary exists between the core and shell. With the increase of shell thickness to ~7.5 monolayers of ZnS as in our CdZnS/ZnS AS QDs, it is expected that dislocations will be formed if the core-shell interface were sharp. As a reference, for CdSe/CdS QDs with core-shell lattice match of ~3.8%, dislocations will be formed as the shell thickness exceeds 4-5 monolayers of CdS [3]. However, the high resolution TEM image of our CdZnS/ZnS AS CQDs manifests high crystallinity across the whole QD without any observable dislocations, which indicates that the interface is not sharp but alloyed in our CdZnS/ZnS AS CQDs.

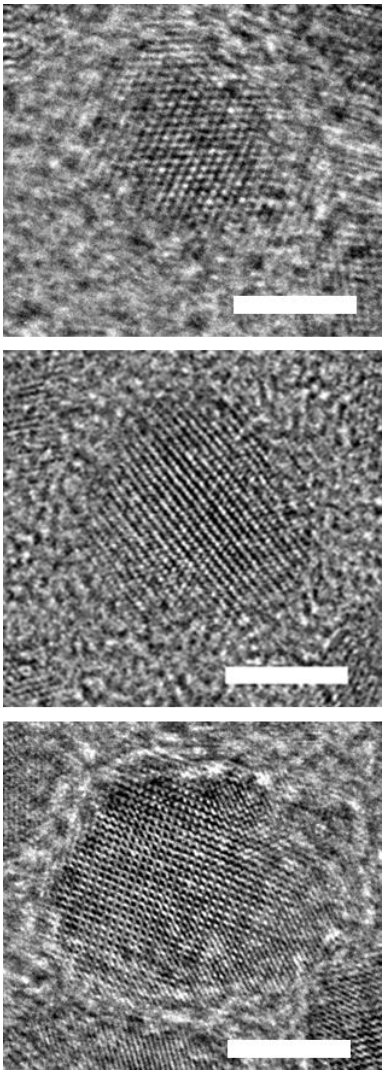

Figure S2. High resolution TEM images of CdZnS core (top), CdZnS/ZnS SS (middle) and CdZnS/ZnS AS (bottom) CQDs. Scale bar is 5 nm.

To study the influence of the variation in stimulated emission threshold by change of absorption, the absorption of the thin films of CdZnS core, CdZnS/ZnS SS and CdZnS/ZnS AS QDs used in the stimulated emission investigation were measured. Based on the same preparation conditions (spin coating speed, solution mass concentration (~30 mg/mL), thin films with similar thicknesses were produced, as is shown by the scanning electron microscopy (SEM) images of the film cross-section in Figure S3a. The corresponding absorption spectra are displayed in Figure S3b. The absorbance of CdZnS/ZnS AS QDs is found to only increase ~17% and ~38% at excitation wavelength of 400 nm compared to that of CdZnS/SS QDs and CdZnS core, respectively.

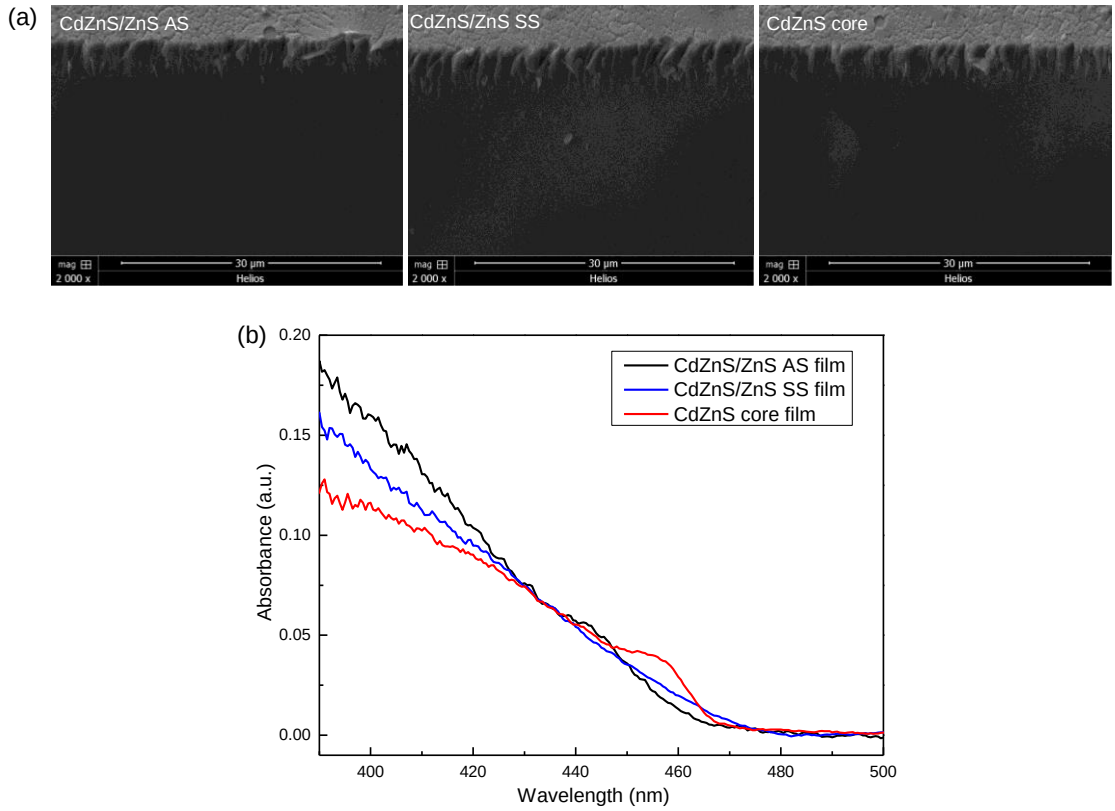

Figure S3. (a) Cross section of thin films of CdZnS/ZnS AS QDs, CdZnS/ZnS SS QDs and CdZnS core viewed under scanning electron microscopy (SEM). 25 nm-thick Au was coated to reduce charging effects. (b) Absorption spectra of the thin

films of CdZnS/ZnS AS QDs, CdZnS/ZnS SS QDs and CdZnS core.

Figure S4 shows the transmission spectrum of the distributed Bragg reflector (DBR) substrate. The stop-band width of Bragg reflector is about 140 nm with reflectivity of about 99.5% at 460 nm.

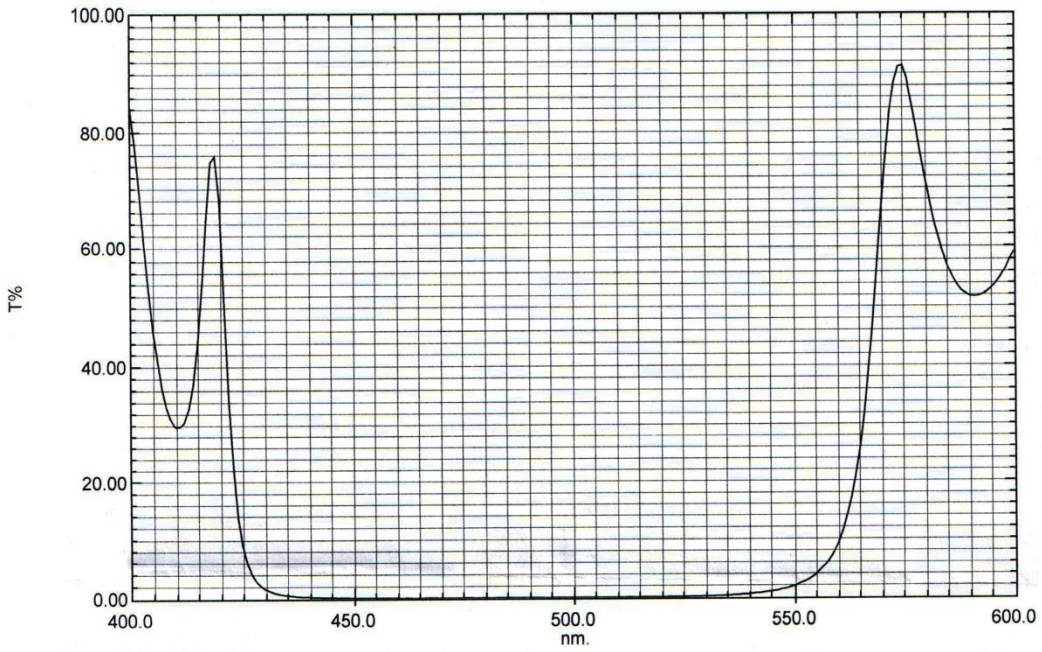

Figure S4. Transmission spectrum of the distributed Bragg reflector substrate.

Figure S5a shows the overview image of the microplotter system used for the quai-toriod microlaser fabrication. Figure S5b examplify the optical image of the quasi-toroid microlasers with various sizes produced by the microplotter system.

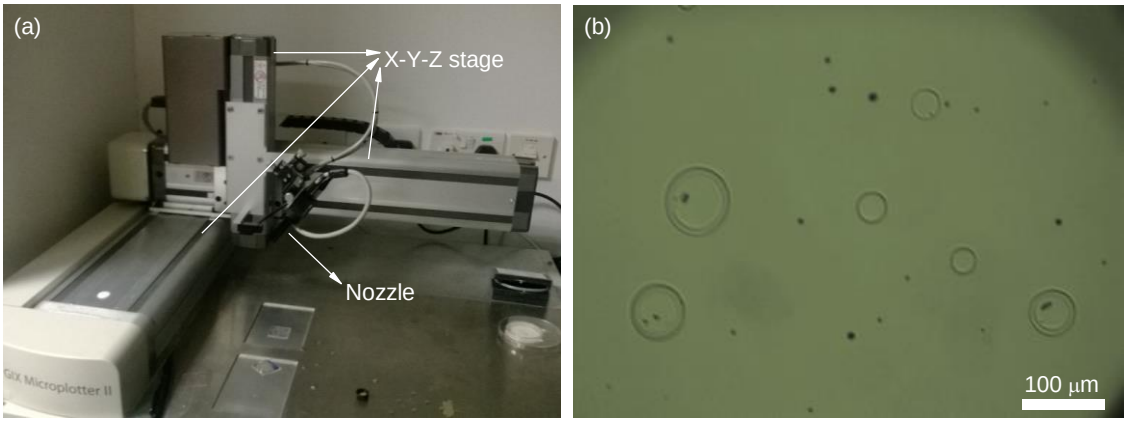

Figure S5. (a) Image of the microplotter system. (b) Quasi-toroid lasers with various sizes fabricated by the microplotter system.

Figure S6a presents the atomic force microscopy (AFM) image recorded in tapping of the ring wall, and the cross section profile of the ring wall is presented in Figure S6b. A pretty smooth surface and well-defined border of the ring wall are revealed.

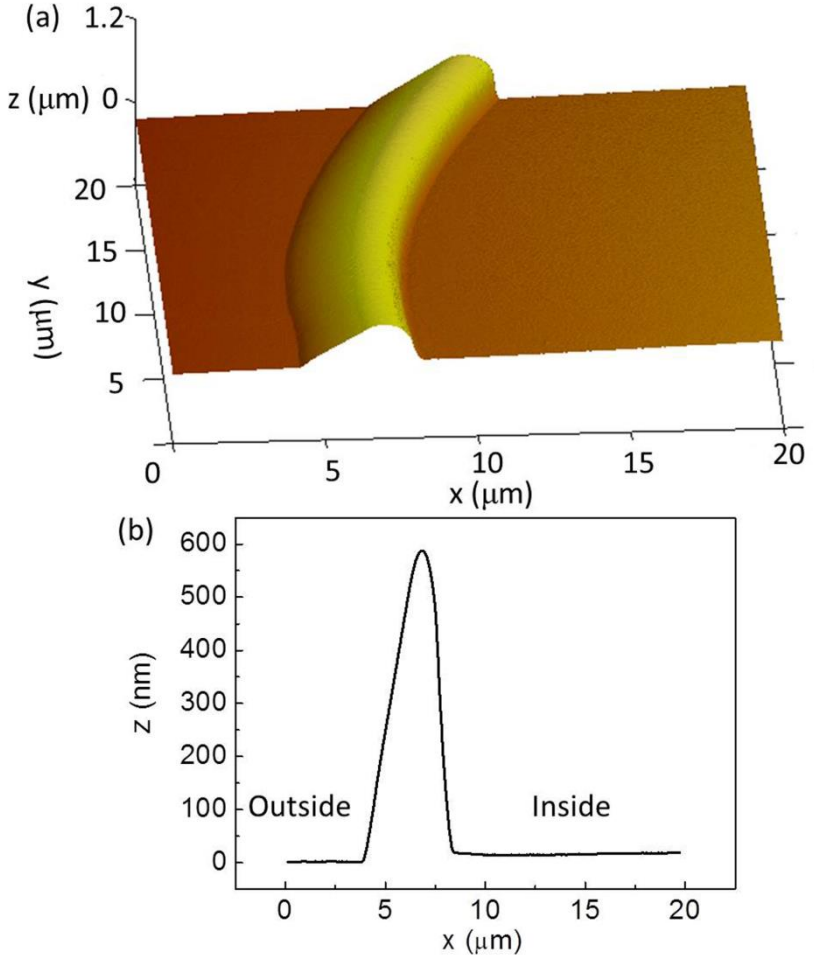

Figure S6. (a) Atomic force microscopy image recorded in tapping mode around the ring wall. (b) Cross section profile of the ring wall.

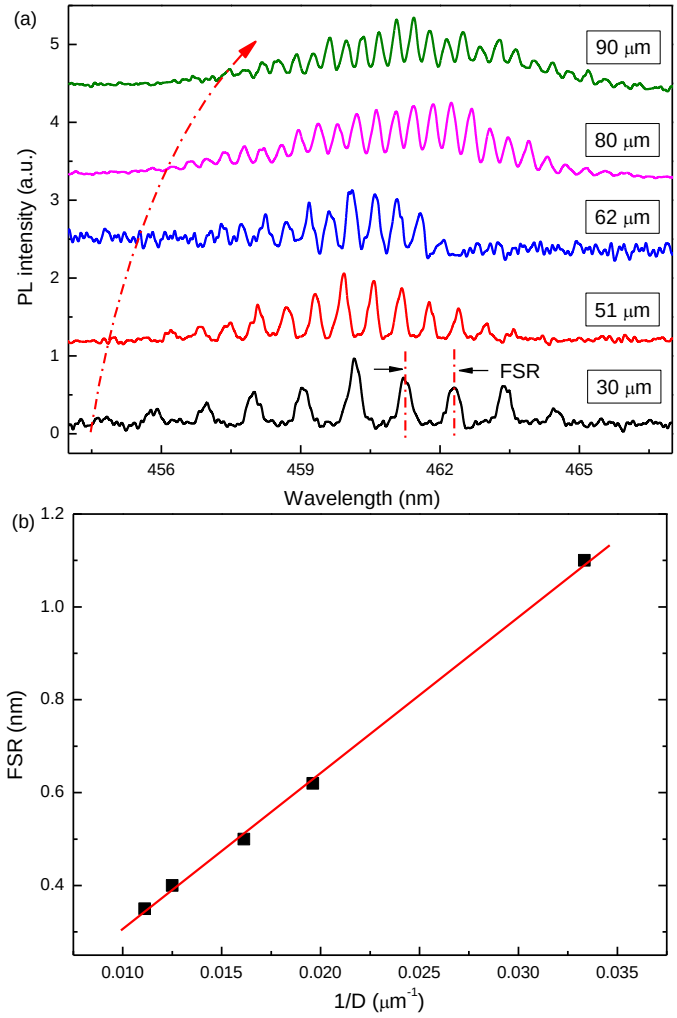

Figure S7. (a) Lasing spectra of various sized quasi-toroid microlasers, indicating that the free spectral range (FSR) decreases with the reduction of the quasi-toroid size. (b) FSR is found to be in inverse proportion to the diameter of the quasi-toroid lasers, confirming the whispering gallery mode lasing mechanism of the quasi-toroid microlasers.

References:

1. Shen, H.; Bai, X.; Wang, A.; Wang, H.; Qian, L.; Yang, Y.; Titov, A.; Hyvonen, J.; Zheng, Y.; Li, L. S. Adv. Funct. Mater. 24,2367-2373 (2014).
2. Shen, H.; Cao, W.; Shewmon, N. T.; Yang, C.; Li, L. S.; Xue, J. Nano Lett. 15,1211-1216 (2015).
3. Nan, W.; Niu, Y.; Qin, H.; Cui, F.; Yang, Y.; Lai, R.; Lin, W.; Peng, X. J. Am. Chem. Soc. 134,19685-19693 (2012).